Journal of Mechanical and Energy Systems (JMES)

Volume xx Nomor xxx 2024

NUMERICAL SIMULATION OF DIMETHYL ETHER/AIR PREMIXED FLAMES

Aris Purwanto[1*], Lin Po-Hung[2]
[1] Dept of Mechanical Engineering, Universitas Negeri Surabaya, Indonesia
[2]Department of Aeronautics and Astronautics, National Cheng Kung University, Tainan, Taiwan

*Corresponding author
arispurwanto@unesa.ac.id

Graphical abstract

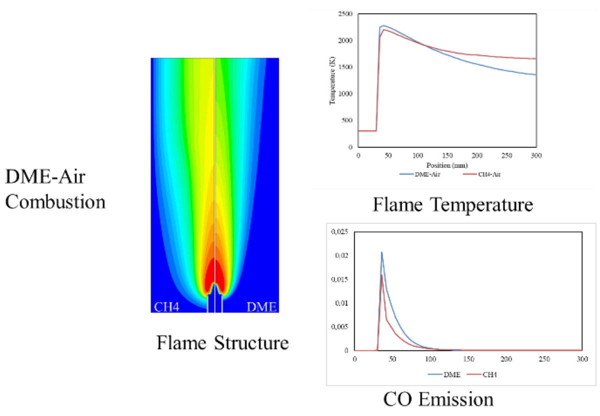

Abstract

The increasing global demand for energy necessitates the development of cleaner and more environmentally sustainable alternative fuels. Dimethyl ether (DME) is identified as a promising candidate due to its high internal oxygen content and favorable combustion properties. The present study investigates the combustion characteristics of a DME–air mixture and compares them with those of a CH_4–air mixture using Computational Fluid Dynamics (CFD) simulations in ANSYS Fluent. Simulations were conducted for a tube with an 11.5 mm diameter and a 300 mm length under laminar flow conditions. Key parameters analyzed include temperature distribution and the mole fractions of CO and CO_2 throughout the combustion domain. The results show that the DME–air mixture demonstrates a more rapid initial temperature increase in the flame zone, although it attains a slightly lower maximum temperature than the CH_4–air mixture. CO formation in DME is initially higher but decreases more rapidly due to a more efficient oxidation process to CO_2. In contrast, CO formation in CH_4 is slower but persists longer within the domain. The CO_2 mole fraction distribution indicates that DME produces CO_2 more rapidly at the onset of combustion, whereas CH_4 displays a more gradual and steady increase. These findings suggest that DME exhibits more reactive, efficient combustion characteristics for converting CO to CO_2, underscoring its significant potential as a cleaner, more sustainable alternative to conventional methane-based fuels.

Keywords: Dimethyl Ether (DME); CH_4; Laminar Combustion; CFD; ANSYS Fluent; Temperature; CO Emission; CO_2 Emission

© 2024 Publisher: Mechanical Engineering Study Program, UNESA

Article history : Received, 2 Maret 2025, Received in revised: 15 Juni 2025, Accepted; 25 Juni 2025, Published online: 30 Juni 2025

1. Introduction

The rapid increase in global energy demand has prioritized the development of clean, sustainable, and environmentally friendly energy sources [1]. Nevertheless, fossil fuels such as gasoline and diesel continue to dominate the energy sector because of their high energy density, established infrastructure, and relatively low cost [2]. Combustion of these conventional fuels generates significant quantities of harmful emissions, including nitrogen oxides (NOx), carbon monoxide (CO), unburned hydrocarbons (UHC), and soot particles, which contribute to air pollution, global warming, and adverse health effects [3], [4], [5]. These environmental and health concerns have intensified efforts to identify alternative fuels that provide high efficiency with minimal emissions [6], [7].

Dimethyl Ether (DME) has emerged as a particularly promising alternative fuel. DME (CH3OCH3) is a simple oxygenated hydrocarbon characterized by a high cetane number (55–60), excellent ignition quality, and the absence of carbon–carbon bonds, which prevents soot formation during combustion [8], [9], [10]. Additionally, DME exhibits favorable physical properties, including high vapor pressure and low boiling point, which facilitate easy atomization and thorough mixing with air [11]. These attributes make DME suitable for use in both compression-ignition (CI) engines and gas-turbine combustion systems. DME can be synthesized from a range of feedstocks, including natural gas, coal, and renewable biomass, via synthesis gas (syngas) intermediates, providing flexibility for integration with existing energy infrastructures [12], [13], [14]. When produced from renewable sources, DME is considered a carbon-neutral fuel that can significantly reduce lifecycle greenhouse gas (GHG) emissions. Its clean-burning properties and compatibility with current engine technologies position DME as a strong candidate for the transition to sustainable energy systems [15].

Despite these advantages, the combustion characteristics of DME—including flame structure, emission formation, and flame stability under varying operating conditions—remain complex and not fully understood. Computational Fluid Dynamics (CFD) has emerged as a powerful tool for investigating combustion phenomena. CFD integrates fluid dynamics, turbulence, heat transfer, and chemical kinetics to predict detailed combustion behavior with high spatial and temporal resolution. Using CFD simulations, it is possible to systematically analyze the effects of parameters such as equivalence ratio, inlet velocity, and burner geometry on flame temperature distribution, species concentration, and pollutant formation. This study aims to conduct a numerical investigation of DME–air combustion using CFD to examine the effects of key operating parameters on flame characteristics and emission behavior. The insights obtained are expected to inform the design of efficient, stable, and environmentally friendly DME-fueled combustion systems.

2. Material and Method

2.1 Numerical Approach

This study investigates the combustion behavior of Dimethyl Ether (DME)–air mixture using Computational Fluid Dynamics (CFD) with ANSYS Fluent 2020. The simulations were carried out under steady-state, laminar, reacting-flow conditions to analyze the flame structure, temperature distribution, and emission characteristics. The laminar model was selected because the Reynolds number in the burner configuration is low, ensuring the flow remains fully laminar throughout the domain [16]. Two-dimensional Computational Fluid Dynamics (CFD) simulations were conducted to capture the spatial distribution of flow and reactive species, CFD software was widely used for the combustion phenomena [17], [18]. In this study, to reduce computational cost, a two-dimensional configuration was employed. The ANSYS Fluent software was used for numerical simulations. The simulations were performed on an Intel Core i7 computer with 16 GB of RAM. SIMPLE Algorithm with pressure-based solver was used in this simulation, The governing equations consist of the steady-state, two-dimensional Navier–Stokes equations, along with conservation equations for mass, energy, and species transport for all participating chemical species [19]. This simulation also operated under the following assumptions: (1) steady-state combustion, (2) Dufour and Soret effects neglected, (3) gas radiation neglected, (4) laminar flow, and (5) incompressible flow with ideal gas conditions. Based on all these assumptions, the conservation equations are formulated:

Continuity Conservation

$$\frac{\partial(\rho u)}{\partial x}+\frac{\partial(\rho v)}{\partial r}+\frac{\rho v}{r}=0 \tag{1}$$

Momentum Equations

Axial Direction

$$\rho u\frac{\partial u}{\partial x}+\rho v\frac{\partial u}{\partial r}=-\frac{\partial p}{\partial x}+\mu\left(\frac{\partial^2 u}{\partial x^2}+\frac{\left(\frac{1}{r}\right)\partial}{\partial r}\left(r\frac{\partial u}{\partial r}\right)\right) \tag{2}$$

Radial Direction

$$\rho u\frac{\partial v}{\partial x}+\rho v\frac{\partial v}{\partial r}=-\frac{\partial p}{\partial r}+\mu\left(\frac{\partial^2 v}{\partial x^2}+\frac{\left(\frac{1}{r}\right)\partial}{\partial r}\left(r\frac{\partial v}{\partial r}\right)-\frac{v}{r^2}\right) \tag{3}$$

Energy Equation

$$\rho u\frac{\partial h}{\partial x}+\rho v\frac{\partial h}{\partial r}=\nabla\cdot(k\nabla T)+\Sigma\, h_{\mathrm{i}}\,\dot{\omega}_{\mathrm{i}} \tag{4}$$

Species Transport Equation

$$\rho u\frac{\partial Y_{\mathrm{i}}}{\partial x}+\rho v\frac{\partial Y_{\mathrm{i}}}{\partial r}=\nabla\cdot(\rho D_{\mathrm{i}}\,\nabla Y_{\mathrm{i}})+\dot{\omega}_{\mathrm{i}} \tag{5}$$

2.2 Geometry and Computational Domain

A two-dimensional axisymmetric burner geometry was developed to model a laminar premixed DME–air flame. The computational domain consisted of a cylindrical chamber with a diameter of 11.5 mm and a length of 300 mm, as shown in **Figure 1**. These dimensions were chosen to ensure a fully developed flame and to minimize boundary effects on the outlet flow. The geometry was designed in ANSYS DesignModeler, and the mesh was generated in ANSYS Mesher, with fine refinement in the flame zone to capture steep gradients in temperature and species concentrations. A mesh independence test was conducted by comparing the maximum flame temperature and velocity distribution at different grid densities to ensure the accuracy of numerical predictions.

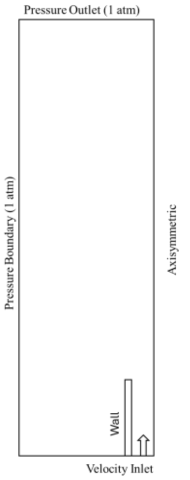

Figure 1 Computational Domain

2.3 Boundary Conditions

The inlet boundary conditions were specified as a uniform velocity inlet with a flow speed of 0.8 m/s with an equivalent ratio of 1. The outlet was defined as a pressure outlet to facilitate pressure-driven flow. Both the inlet and backflow temperatures were maintained at 295 K to simulate ambient conditions. Wall boundaries were assigned a no-slip condition, resulting in zero velocity at the walls to represent viscous effects near solid boundaries accurately.

2.4 Numerical Scheme and Convergence Criteria

The simulations were performed using the pressure-based solver in steady-state mode. Pressure–velocity coupling was handled using the SIMPLE algorithm, while second-order upwind discretization schemes were applied for momentum, energy, and species equations to ensure numerical accuracy [19]. A tetrahedral mesh was used to discretize the computational domain [20]. Mesh refinement was implemented, especially near the wall regions adjacent to the reaction zone, to capture steep gradients in temperature and species concentration. To verify the numerical results' reliability, a grid independence test was performed by varying the mesh size. A refinement size of 0.2 mm produced the most stable results, with deviations of less than 1.8% compared to finer meshes. Simulations were considered converged when the residuals of the governing equations fell below 10−5. This convergence criterion indicates that the iterative solution process achieved sufficient accuracy, as subsequent iterations produced negligible changes.

3. Results and Discussion

Simulation results reveal distinct differences in the combustion characteristics of DME–air and CH_4–air mixtures. Both fuels generate a pronounced flame zone near the nozzle, characterized by a sharp increase in temperature due to the oxidation reaction between the fuel and air. DME–air combustion achieves a maximum temperature of approximately 2250 K, which is marginally higher than the 2180 K observed for CH_4–air combustion. The flame structure of DME-Air, compared with CH4-Air, is shown in **Figure 2**. This temperature disparity suggests that DME is more reactive than methane. The presence of an oxygen atom in the DME chemical structure promotes radical formation and accelerates the initial combustion reaction. Consequently, the DME flame is shorter yet more intense near the nozzle. In contrast, CH_4–air combustion produces a more extended, more stable temperature profile. This outcome is attributed to the slower reaction rate of methane, which permits the oxidation process to proceed gradually throughout the combustion domain. The slower decrease in temperature in the CH_4–air mixture indicates a more uniform release of thermal energy along the flow path. Overall, DME demonstrates the capacity to achieve higher peak temperatures and faster reaction rates than methane. However, DME flames are typically shorter due to the rapid onset of combustion. These findings suggest that DME has significant potential as an efficient, environmentally friendly alternative fuel, particularly for combustion systems that demand high efficiency and short reaction times, the flame temperature was shown in **Figure 3.**

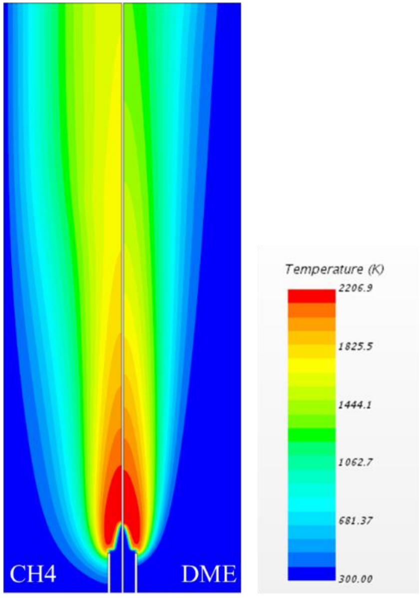

Figure 2 Flame structure of DME-Air compared with CH4-Air

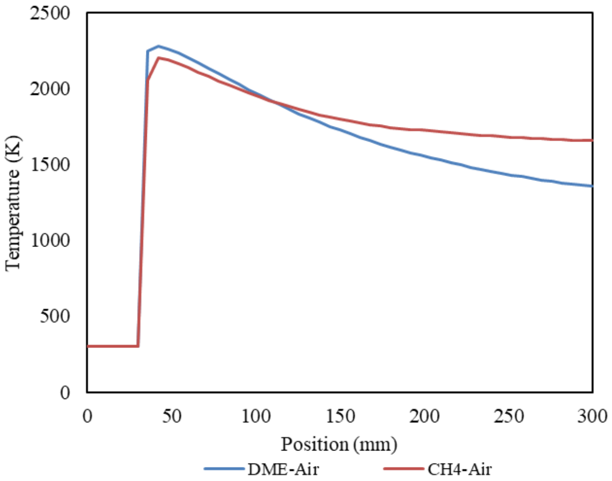

Figure 3 Flame Temperature of DME-Air compared with CH4-Air

Simulation results indicate that carbon monoxide (CO) formation during DME–air and CH_4–air combustion follows distinct trends along the flow direction, as shown in **Figure 4**. At the onset of the combustion zone near the nozzle, both fuels display low CO mass fractions. This outcome is attributed to combustion conditions dominated by complete oxidation, in which most carbon is directly converted to carbon dioxide (CO_2). As the distance from the nozzle increases, CO concentration rises due to decreasing oxygen availability in the flame zone. For the DME–air mixture, the CO mass fraction rises more rapidly and attains a higher maximum value than in CH_4–air combustion. This trend suggests that DME combustion is more reactive in the initial zone, though some of the fuel is not fully oxidized to CO_2. The presence of oxygen within the DME molecular structure promotes the formation of intermediate radicals such as CH_2O and HCO_2, which subsequently contribute to elevated CO concentrations during the initial reaction stage. Consequently, the CO distribution in DME–air combustion is higher near the flame zone than in methane combustion. In contrast, the CH_4–air mixture demonstrates slower CO formation with a lower peak concentration. This behavior is attributed to methane's more stable reaction rate, which facilitates complete and more uniform oxidation throughout the combustion domain. The gradual decrease in CO concentration over extended distances further indicates a more efficient conversion of CO-to-CO_2. Thus, although DME combustion generates higher temperatures and faster reaction rates, it also tends to produce higher CO concentrations in the initial stages due to its intense, rapid reaction characteristics.

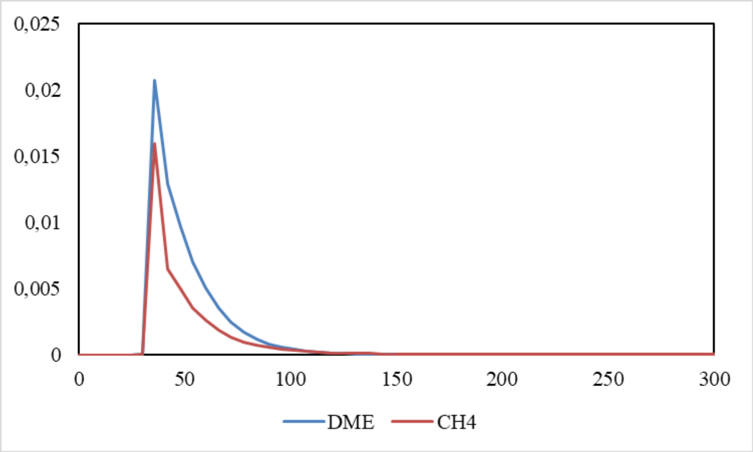

Figure 4 CO Emission of DME-Air compared with CH4-Air

The simulation results show that the CO_2 mole fraction begins to increase significantly after the initial flame zone, with notable formation at approximately 30 mm from the nozzle (see **Figure 5**). Before this point, the CO_2 mole fraction remains low due to incomplete fuel oxidation. The reactions are primarily characterized by the presence of intermediate radicals such as CH_2O and CO. Beyond this distance, the CO_2 mole fraction rises sharply, reaching maximum values of approximately 0.087 for DME–air and 0.112 for CH_4–air at positions around 54–60 mm from the nozzle. The rapid increase in CO_2 for the DME–air mixture suggests an intense oxidation process in the initial flame zone. The internal oxygen content in DME's chemical structure accelerates the formation of intermediate radicals, leading to earlier CO_2 production. After reaching its peak, the CO_2 mole fraction for DME–air gradually decreases to approximately 0.062 at the end of the domain (300 mm), indicating that most oxidation reactions are completed upstream and the downstream CO_2 concentration stabilizes. In the CH_4–air mixture, the increase in CO_2 is more gradual and reaches a slightly higher maximum value than in the DME–air mixture. This trend suggests that methane combustion is more stable and uniform throughout the domain. The simpler molecular structure of CH_4 results in slower decomposition into CO_2, leading to a more even distribution of carbon dioxide along the reaction pathway. Overall, these findings demonstrate that DME generates CO_2 more rapidly but with a faster decline, whereas CH_4 produces CO_2 at a slower yet more consistent rate, reflecting the distinct combustion kinetics of each fuel.

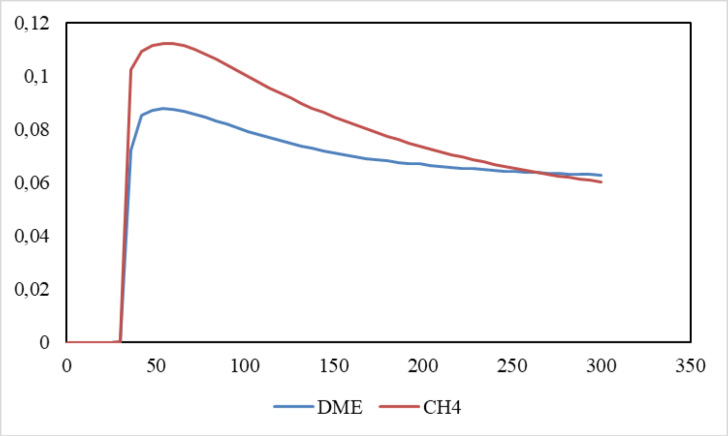

Figure 5 CO_2 Emission of DME-Air compared with CH4-Air

4. Conclusion

Numerical simulations using ANSYS Fluent were conducted to analyze the combustion of Dimethyl Ether (DME)–air and methane (CH_4)–air mixtures under laminar flow conditions in a tube with a diameter of 11.5 mm and a length of 300 mm. The results demonstrate significant differences in the combustion characteristics of the two fuels. The DME–air mixture exhibits a slightly lower maximum temperature compared to CH_4–air; however, the temperature rise occurs more rapidly in the initial flame zone. This behavior suggests that DME is more reactive, due to the presence of oxygen atoms in its molecular structure, which facilitates combustion initiation. During DME combustion, the initial CO concentration is higher due to incomplete oxidation, but it decreases more rapidly than in CH_4 combustion as CO is converted to CO_2 more efficiently. In contrast, CH_4 combustion produces lower initial CO concentrations, but these persist longer throughout the reaction domain. The CO_2 mole fraction results show that DME produces CO_2 more rapidly at the beginning of the combustion zone, but the rate decreases more quickly after reaching the peak. At the same time, CH_4 produces CO_2 more gradually with a more even distribution downstream of the domain. Overall, it can be concluded that DME combustion is more reactive and efficient in converting CO to CO_2, although its maximum temperature is slightly lower. This shows the great potential of DME as a cleaner, more environmentally friendly alternative to methane.

Reference

[1] G. Li, Z. Zhu, Y. Zheng, W. Guo, Y. Tang, and C. Ye, "Experiments on a powerful, ultra-clean, and low-noise-level swirl-combustion-powered micro thermoelectric generator," *Energy*, vol. 263, p. 125825, 2023, doi: https://doi.org/10.1016/j.energy.2022.125825.

[2] B. Aravind, B. Khandelwal, P. A. Ramakrishna, and S. Kumar, "Towards the development of a high power density, high efficiency, micro power generator," *Appl Energy*, vol. 261, p. 114386, 2020, doi: https://doi.org/10.1016/j.apenergy.2019.114386.

[3] A. Fayyazbakhsh *et al.*, "Engine emissions with air pollutants and greenhouse gases and their control technologies," *J Clean Prod*, vol. 376, p. 134260, 2022, doi: https://doi.org/10.1016/j.jclepro.2022.134260.

[4] G. Ospina, M. Y. E. Selim, S. A. B. Al Omari, M. I. H. Ali, and A. M. M. Hussien, "Engine roughness and exhaust emissions of a diesel engine fueled with three biofuels," *Renew Energy*, vol. 134, pp. 1465–1472, 2019.

[5] M. Rabe *et al.*, "Comparative Analysis on the Performance and Exhaust Gas Emission of Cars with Spark-Ignition Engines," *Energies (Basel)*, vol. 15, no. 17, p. 6361, 2022, [Online]. Available: https://www.mdpi.com/1996-1073/15/17/6361

[6] Y.-H. Li, S. Pangestu, A. Purwanto, and C.-T. Chen, "Synergetic combustion behavior of aluminum and coal addition in hybrid iron-methane-air premixed flames," *Combust Flame*, vol. 228, pp. 364–374, 2021, doi: https://doi.org/10.1016/j.combustflame.2021.02.013.

[7] Y.-H. Li, A. Purwanto, and B.-C. Chuang, "Micro-Explosion mechanism of iron hybrid Methane-Air premixed flames," *Fuel*, vol. 325, p. 124841, 2022, doi: https://doi.org/10.1016/j.fuel.2022.124841.

[8] Z. Azizi, M. Rezaeimanesh, T. Tohidian, and M. R. Rahimpour, "Dimethyl ether: A review of technologies and production challenges," *Chemical Engineering and Processing: Process Intensification*, vol. 82, pp. 150–172, 2014.

[9] D. Liuzzi, C. Peinado, M. A. Pena, J. van Kampen, J. Boon, and S. Rojas, "Increasing dimethyl ether production from biomass-derived syngas via sorption enhanced dimethyl ether synthesis," *Sustain Energy Fuels*, vol. 4, no. 11, pp. 5674–5681, 2020.

[10] J. Chang, Y. Fu, and Z. Luo, "Experimental study for dimethyl ether production from biomass gasification and simulation on dimethyl ether production," *Biomass Bioenergy*, vol. 39, pp. 67–72, 2012.

[11] H. Saputro, L. Fitriana, A. Purwanto, R. Muslim, F. A. Munir, and W.-C. Wang, "The effect of natural waste filter on dimethyl ether production from low calorific coal gasification," *Clean Eng Technol*, vol. 21, p. 100772, 2024, doi: https://doi.org/10.1016/j.clet.2024.100772.

[12] K. Sun, W. Lu, F. Qiu, S. Liu, and X. Xu, "Direct synthesis of DME over bifunctional catalyst: surface properties and catalytic performance," *Appl Catal A Gen*, vol. 252, no. 2, pp. 243–249, 2003.

[13] A. Aloise *et al.*, "Desilicated ZSM-5 zeolite: Catalytic performances assessment in methanol to DME dehydration," *Microporous and mesoporous materials*, vol. 302, p. 110198, 2020.

[14] Z. Wang *et al.*, "Design and operation of a pilot plant for biomass to liquid fuels by integrating gasification, DME synthesis and DME to gasoline," *Fuel*, vol. 186, pp. 587–596, 2016.

[15] Y. Li, S. Su, L. Wang, J. Yin, and S. Idiaba, "Reduction and optimization for combustion mechanism of dimethyl ether–air mixtures," *Int J Chem Kinet*, vol. 54, no. 3, pp. 142–153, 2022.

[16] A. Purwanto, H. Saputro, A. F. Alhikami, and F. A. Munir, "Enhancing Stoichiometric Methane-Air Flames: The Role of N2O Replacement," *Automotive Experiences*, vol. 8, no. 2, 2025.

[17] H. Saputro *et al.*, “Numerical simulation of flame stabilization in meso-scale vortex combustion,” *MATEC Web of Conferences*, vol. 197, 2018, doi: 10.1051/matecconf/201819708005.

[18] H. Saputro, L. Fitriana, A. Purwanto, F. A. Munir, and W.-C. Wang, “A Development of Meso-Scale Vortex Combustion for a Micro Power Generator Based on a Thermoelectric Generator,” *Fluids*, vol. 7, no. 12, p. 386, 2022, [Online]. Available: https://www.mdpi.com/2311-5521/7/12/386

[19] Inc. ANSYS, *ANSYS Fluent Theory Guide Release 15*. 2013.

[20] Inc. ANSYS, *ANSYS Meshing User’s Guide*. 2013.